Adaptive Beam Management in 5G-NR: A Machine Learning Perspective

Boqiang Wang
bo6676wa-s@student.lu.se

Department of Electrical and Information Technology
Lund University

Supervisor: Harsh Tataria

Examiner: Fredrik Rusek

March 24, 2021

Printed in Sweden
Tryckeriet i E-huset, Lund

Abstract

In this rapid era of technology, speed of communication has become an important factor. To overcome this challenge, 5G/NR technology is being explored. One of the ways of doing this is by using the so called millimeter wave spectrum. In order to make usage of the mmWave spectrum, due to the high path loss it introduces, the beamforming technique is adopted. Beamforming is a method used in high frequency signal transmission for focusing or directing the beam towards the user in such a way that it will improve the signal strength and throughput and reduce the signal wastage, resulting in better experience. This can be achieved by constructively adding the phase shift from each antenna element towards the desired direction. Beam refinement or tracking, which are used in 5G/NR, are the mechanisms that selects the active beam used for transmission between the base station and User Equipment. Beam management is based on the continuous measurement reports from the UE on the reference signals related to the available beams. With higher frequencies and more narrow beams for coverage enhancements, beam management is becoming increasingly important. However, it comes with a collective cost due to the frequent measurements that are needed to monitor the positions of all connected UEs.

The purpose of this Master's thesis work is to investigate if machine learning methods could be applied to optimize the beam measurements and find the most efficient way to use these results to select the best beam for multiple UEs. This will allow the UEs and Base Station (BS) to have a strong signal for better transmission. We further compare the results obtained, with 3GPP baseline algorithm to gain insights about its performance.

Acknowledgements

At the beginning, I would like to express my gratitude towards Ericsson AB for offering me such an opportunity to write thesis there. Also, I want to give big thanks to Marcus Davidsson and Michail Triantafyllidis who have been my supervisors at Ericsson AB for providing me tons of helps and suggestions about my thesis. Meanwhile, I send out the special thanks to Professor Harsh Tataria who is the university supervisor at LTH for giving me productive feedbacks and guidance.

Table of Contents

List of Figures

List of Tables

Chapter 1

Introduction

1.1 Background and Motivation

The high data rate transmission is now one of the most import requirements for the Mobile technology. There is no doubt that the Fifth Generation New Radio (5G NR) technology can support higher bandwidth and throughput compared to the Fourth Generation 4G. In order to accomplish this purpose, many technologies and features are applied into 5G NR. For example, the millimeter wave (mmWave) spectrum, which enables much higher data rate transmission for 5G with respect to huge bandwidth benefit. However, the millimeter wave (mmWave) spectrum uses extremely high frequency, which results in big propagation loss and some other problems (e.g. mmWave is more prone to fading). To overcome this big disadvantage, beamforming is applied in 5G. The purpose of beamforming is that the transmitter (gNodeB) can concentrate the signal energy to the receivers (UEs). In order select and retain the most suitable beam pairs, beam management is needed, which consists of beam establishment, beam refinement and beam tracking. The perfect beam alignment between a transmitter and an intended receiver requires an intelligent and adaptive beam measurement algorithm, which can accurately and efficiently select the best beam pair based on the mobility of the receiver.

1.2 Project Aims

The purpose of this Master thesis work is to investigate the impact of using machine learning method, more specifically neural network, which can potentially deal with a certain isolated sub-task within the general framework of optimized beam measurements for 5G NR. The studied sub-task concerns selection of best narrow beam for single and multiple UEs, which will be carefully defined in later sections.

1.3 Methodology

In order to accomplish the project aims, the author started with a literature study. Author completed a Neural network online course by Professor Andrew Ng in Stanford University. In this course, the relevant knowledge about functions of neural network is presented. What is more, the corresponding programming exercises were also included. Then the category of data that should be used as input to the machine learning algorithms were collected by using the Ericsson lab simulator in Lund. Data was collected, filtered and used to train neural network in MATLAB. The machine learning algorithm will be compared to the results of the 3GPP baseline algorithm to gain insights about its performance.

1.4 Previous Work

Previous studies have been performed in this area using reinforcement learning (Q-learning) and neural network for tracking the speed of UE, both have shown significant improvements in the result. In the context of this thesis, the beam tracking will be performed using a machine learning algorithm, and its performance will be compared to the baseline beam tracking algorithm.
In research [1], four machine learning algorithms, which are multi-class neural network, binary neural network, logistic regression and support vector machine techniques are used to classify if the UE is moving or is stationary, in spatial beamforming technology. Amplitude samples are collected and displayed clearly in scatter plots. Results from Neural Network are analyzed using confusion matrix. Finally, neural networks are found to be more accurate than the other algorithms. A certain accuracy criterion was defined, which can be found in this research, binary neural network with 98% accuracy and multiclass neural network with 89.2% accuracy when the UE is moving or stationary. Further, logistic regression and support vector machine are implemented to compare with Neural Network, and are found to be less accurate, 95% and 93.8% respectively.
In research [2], authors use machine learning algorithms namely Q-learning, which is reinforcement learning to be applied in the beam management in 5G NR. The algorithm aims to optimize the narrow beam selection, which can provide a better signal quality and higher data throughput. The result is quite promising, but it seems that the throughput improvement is reserved.
In research [3], authors use machine learning algorithms namely Deep learning, which is supervised learning for the beam management in 5G NR. The algorithm aims to help in beam pair selection when beams are misaligned. The result is quite promising, as the prediction accuracy and throughput improvement is obvious.

Chapter 2

Theoretical Background

2.1 5G NR

A new radio access technology (RAT) called 5G NR is developed by the 3rd Generation Partnership Project (3GPP) for the fifth generation mobile network (5G). 5G NR offers globalized standards for the 5G networks with higher capability. 5G NR can provide outstandingly faster mobile experience and can be utilized in many other industries. 5G NR can fulfil the extension and diversity of connection requirements in terms of extremely high throughput, high reliability, low delay, low power consumption as well as flexibility and robustness. 5G NR is featured with many advance technologies, e.g. massive MIMO and beam management [4].

2.2 mmWave Spectrum

The millimeter wave (mmWave) spectrum is above 10GHz, which offers lots of higher bandwidth than LTE or other cellular systems. Consequently, the network can offer high data speed. However, the ultra-high frequency has much worse channel propagation properties compare to the low band transmission. Transmitting in mmWave always suffers from relatively high path loss and it can be easily reflected or absorbed by the surface of many common materials. In addition, the signal strength can drop rapidly due to the different relative positions between body and user equipment (UE). In order to overcome these problems, a high directional connection between mmWave gNB and UE is needed in order to get the advantage of the beamforming gain and keep a decent communication quality. Thus, beam management is required [5].

2.3 OFDM

OFDM (Orthogonal Frequency Division Multiplexing) is a unique frequency division multiplexing (FDM) method. The information is divided into many chunks and transmitted independently in multiple carrier system. The OFDM splits the

channel into many narrow bandwidth sub-channels to carry information. Traditional frequency division multiplexing system needs guard bands between carriers to prevent inter carrier interference (ICI), in which no information can be transmitted. Consequently, the spectral efficiency is low. OFDM solves this problem by using orthogonal subcarriers at the transmitting side, which not only keep subcarriers unrelated and independent, but also let subcarriers overlap each other. So that the guard band is not needed any more. That is the reason why OFDM has very good spectral efficiency. What is more, the OFDM has narrow band subchannels which means the OFDM can overcome channel fading very well compare to the single wide band system. To avoid inter-symbol interference (ISI), a cyclic prefix (CP) is inserted before one symbol, which contains the end section of symbol which will be transmitted as follow. The length of CP is the length of multiple path channel, the CP ensures orthogonality of carriers after channel [6].

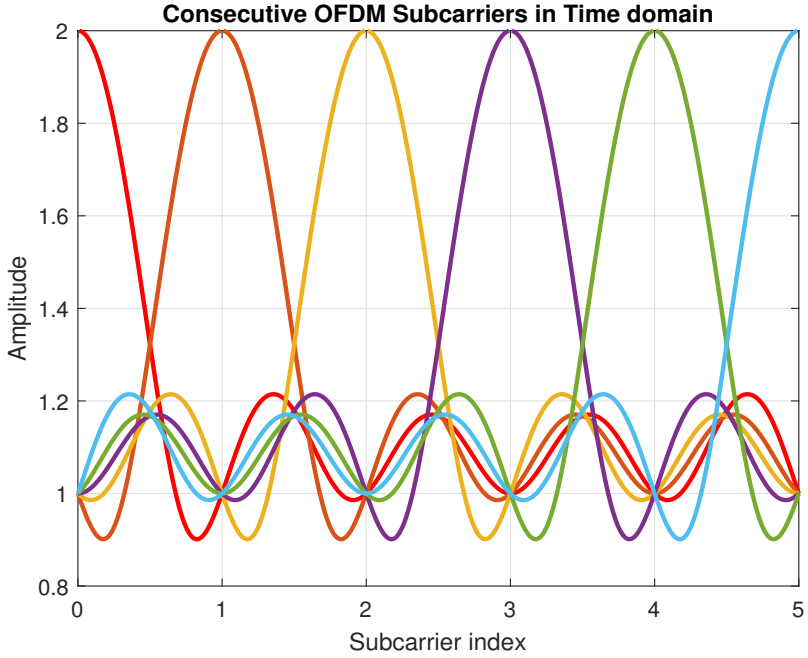

Figure 2.1: OFDM Subcarriers

2.4 Numerology and Frame Structure

3GPP releases the numerology concept for 5G NR, which defines the OFDM system design with respect to Cyclic prefix and subcarrier spacing (SCS). The 5G NR numerology is created for diversity and flexibility purposes in order to satisfy different performance and deployment requirements. Starting with subcarrier spacing (SCS) of 15 kHz, the NR numerology increases with exponentially scalable SCS $15 * 2^{\mu}$, where $\mu = \begin{pmatrix} 0 & 1 & 2 & 3 & 4 \end{pmatrix}$ [7].

μ	0	1	2	3	4
$\Delta f = 2^{\mu} \cdot 15$	15KHZ	30KHZ	60KHZ	120KHZ	240KHZ
OFDM Symbol Duration	$66.67\mu s$	$33.33\mu s$	$16.67\mu s$	$8.33\mu s$	$4.17\mu s$
Cyclic Prefix Duration	$4.69\mu s$	$2.34\mu s$	$1.17\mu s$	$0.57\mu s$	$0.29\mu s$
OFDM Symbol include CP	$71.35\mu s$	$35.68\mu s$	$17.84\mu s$	$8.92\mu s$	$4.46\mu s$
Slot Duration	$1000\mu s$	$500\mu s$	$250\mu s$	$125\mu s$	$62.5\mu s$
Number of slots per subframe	1	2	4	8	16
Number of slots per frame	10	20	40	80	160

Table 2.1: Scalable OFDM numerology for 5G NR

In Figure 2.2, SCS value are presenting in a way of frame structure. The duration of frame is 10ms, and sub-frame duration is 1ms. A sub-frame is then divided into slots consisting of 14 OFDM symbols each. The shorter the slot duration are designed for low delay and high reliability. In comparison, longer slot duration are suitable for low frequency system (larger cell) [8].

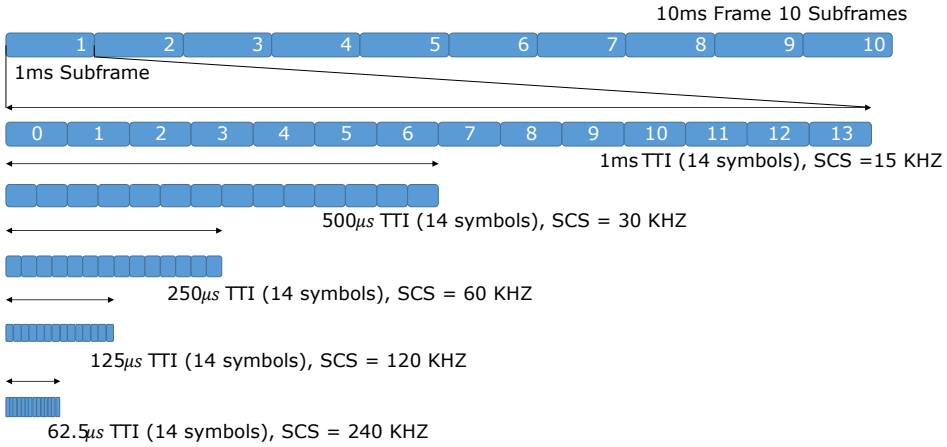

Figure 2.2: Scalable NR TTI.

2.5 MIMO

MIMO can not only improve the performance of cellular system in many ways, but also can fight again multiple path fading with diversity because of the uncorrelated polarization between elements and inter-elements distance. In addition, multiple streams of data can be transmitted by, thus a higher data transmission rate can be achieved due to the spatial multiplexing [9].

2.6 Beamforming

Beamforming enables radio signals transmission to be directional by a steered array of antennas, instead of spreading signals in all directions. By using this technique, antennas can determine the specific direction of stronger beam by distributing and concentrating the energy in one lobe or narrow beam. This technique is commonly used in high data rates wireless communication, because beamforming can maximize the signal transmission efficiency in terms of transmitting and receiving. The benefits that beamforming can bring are higher RSRP and SINR, which is very crucial in 5G broadcast. UEs have strict requirements in terms of coverage and interference as well as SINR, in order to accomplish these requirements, high-precision beamforming is needed to form narrow beams towards multiple UEs, with maximal gains and accurate beam steering. By carefully adjusting and setting the antenna elements, the energy radiation from antenna arrays can be focused into one certain direction which called spatial filtering. Or the receiver antenna arrays can focus on one reception direction. This process is called beamforming. Beamforming can increase the directivity can result in higher link budget. Consequently, the cell coverage and data rates are improved. Meanwhile, the signal interference can be reduced [10].

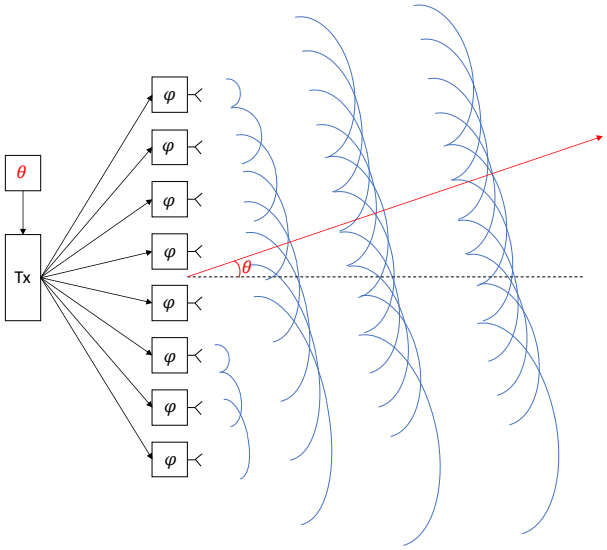

Figure 2.3: Beamforming

2.7 Beam Management

For the data broadcasting and unicasting, the narrow beams must be used in the mmWave system due to the high channel path loss. The task of beam management is to establish a beam pair that can provide good connection based on the circumstances. So, the operations belong to the beam management must be performed

including beam establishment, beam refinement and beam tracking [5].

2.7.1 Beam Establishment

UE acquires broadcast and synchronization information after it powers up, which is the initial process of beam establishment. The Primary Synchronization Signals (PSS) and the Secondary Synchronization Signals (SSS) are two synchronization signals, which help the UE to find and define time slots and subframes as well as the Physical Cell Identity (PCI). The information that UE needs to acquire is sent in the form of blocks which are called SS Block. The beam type used for the establishment procedure is widebeam [11].

2.7.2 Wide Beam Initial selection

Firstly, gNB broadcasts SSBs on each wide beam. Beam sweeps one beam at a time, one SSB index per beam. Secondly, UE measures and selects a suitable beam with a certain SSB index. Thirdly, UE performs random access on RA resources associated with the selected SSB index, Fourthly, depending on the RACH resources the UE utilized, the gNB knows which wide beam the UE selected. Finally, random access procedure completes on the selected wide beam [11].

2.7.3 Beam Refinement

SS Block can be sent through wide beams, while data transmission for the active UE is usually performed through narrow beams, to utilize the beamforming gain. In earlier beam establishment, the beam pair for UE and base station is selected. However, this process doesn't guarantee the best pairing due to the constrained time and resource allocation. NR architecture provides procedure that the beam refinement can be done by providing the down link reference signals (CSI-RS) to the UE. Based on the measurement of these reference signals, gNB can select the corresponding narrow beam. Based on the initial wide beam selection, the gNB firstly transmits CSI-RS on a set of candidate narrow beams. Secondly, The UE measures the CSI-RS signals reports for N CSI-RS resources. Finally, the gNB selects a narrow beam and starts transmitting data to the UE on this narrow beam [12].

2.7.4 Beam Tracking

The Beam Tracking technique assures that the best beam pair for data transmission is maintained when the UE moves, or its environment changes. The base station periodically broadcasts SSBs from which the UE can obtain beam strength (RSRP value) by measuring the SSB signal. The UE reports the measured beam strength value back to the gNodeB, which in turn can decide the best transmission beam. The beam tracking procedure is responsible for both widebeam and narrowbeam changes. The beamtracking is using techniques to detect the strongest narrow beam based on UE measurements for both CSI-RS resources and SSBs [13].

2.8 RSRP

RSRP is calculated per each gNB (DL) reference signal available at a given location. Based on this information it's possible to choose an gNB with the best channel quality to serve an UE. RSRP is the average power value of the resource elements (REs) that contain specified reference signals in a measurement frequency bandwidth. In another word, RSRP is the power value of symbols that only carry resource elements. RSRP can offer the strength of desired signal which can be measured by UE based on the direction from gNB. SS-RSRP (SS reference signal received power) is the average power value over the resource elements that carry secondary synchronization signals(SSS). The measurement time is restricted within the SS/PBCH Block Measurement Time Configuration (SMTC) window duration. CSI-RSRP (CSI reference signal received power) is the average power value over the resource elements that carry CSI-RS signals configured for RSRP measurements [14] [15].

2.9 SSB

The Synchronization Signal Blocks (SSBs) is broadcasted periodically by gNodeB. SSBs consists of Primary Synchronization Signal (PSS), Physical Broadcast Channel (PBCH), Secondary Synchronization Signal (SSS). The UE detects the PSS to require the Physical Cell ID and symbol timing in the SSBs broadcast. From the SSS, UE can get the frame timing and CP length.
DMRS (associated with the PBCH) refers to demodulation reference signal, which is specific for estimate the radio channel. After decoding the DMRS the UE can measure the reference signal received power (RSRP) of different candidate SSB. Based on the measurement, the UE can decide which SSB is the strongest one. The gNB broadcasts SSBs as shown in Fig. 2.5, which are used to do beam sweeping (one SSB per beam). The network sets the periodicity of the SSB. In the default setting, the interval of SSB burst is 20ms(2 NR frames), and the SSB bursts set take 5ms [16].

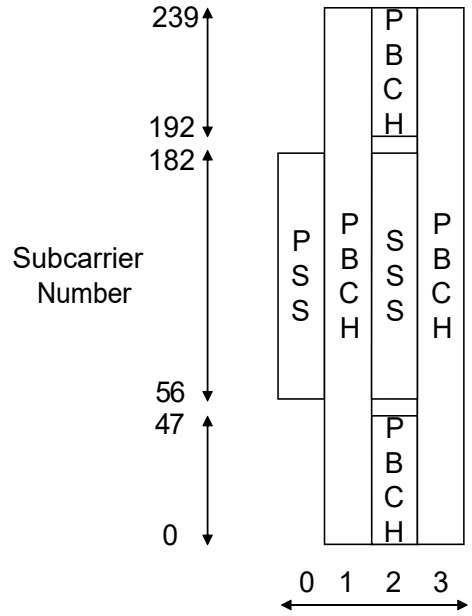

Figure 2.4: SSB Structure

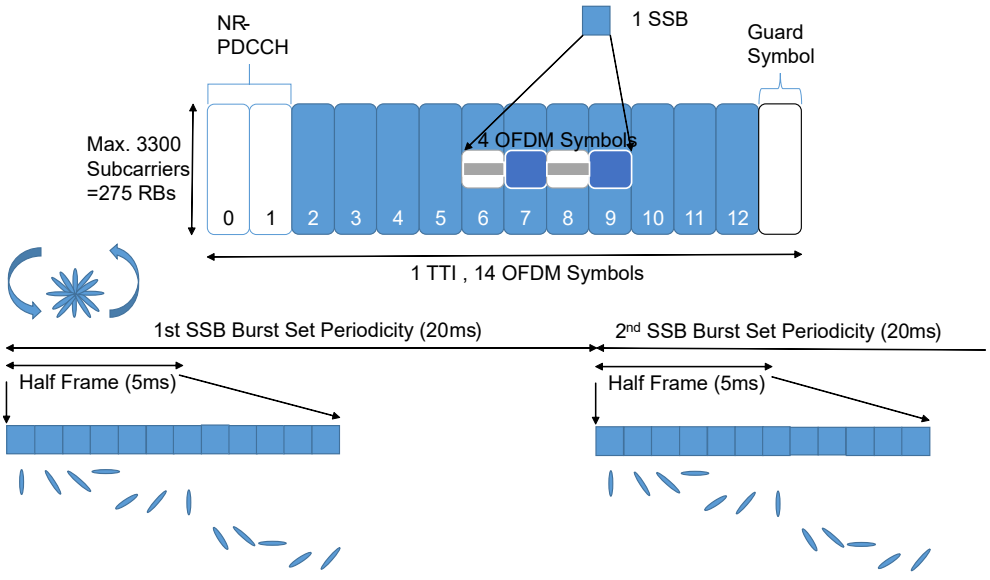

Figure 2.5: SSB Burst

2.10 CSI-RS

UE uses CSI-RS to estimate channel and send the report back to gNodeB. The UE calculate the DL CSI-RS signal and report the CSI measurement in UL. The measurement can be used for mobility check and beam management. CSI-RS has three different types: periodic, semi-persistent or Aperiodic [17].

2.11 Angle of Arrival

Angle of arrival (AoA) has the direction of a received wave by an antenna array. The Angle of Arrival measurement can be done by calculating the time difference of arrival (TDOA) between antenna elements. By calculating the phase difference of received signal at each antenna element, the TDOA can be measured [18].

2.12 Timing Advance

It is vital to ensure the synchronization of downlink and uplink subframes between UE and gNodeB. The UE far away from gNodeB are suffering from more propagation delay compare to the UE closer to gNodeB. UE can adjust its transmission timing by having the Timing Advance value [19].

2.13 Downlink/Uplink Physical Channel

The 5G physical channels contains data over radio interface, which are mapped from higher channels. The physical channel carries payload data and specific data like reference signal and modulation. In this section, three important types of physic channel will be introduced, which are strongly relevant to this thesis [20].

2.13.1 PDSCH

Physical downlink shared channel (PDSCH) carries a variety of payload, which are user data, Higher layer control message and system information blocks. In addition, PDSCH also carries Channel state information reference signal (CSI-RS) for beam management.

2.13.2 PDCCH

Physical downlink control channel (PDCCH) contains scheduling signal for PDSCH and PUSCH.

2.13.3 PUSCH

Physical uplink shared channel (PUSCH) carries user uplink data. And, user uses PUSCH to report CSI in periodic or aperiodic manner.

One of most common patterns of TDD physical channel is 4-1 pattern, which denotes four downlink slots and one uplink slot.

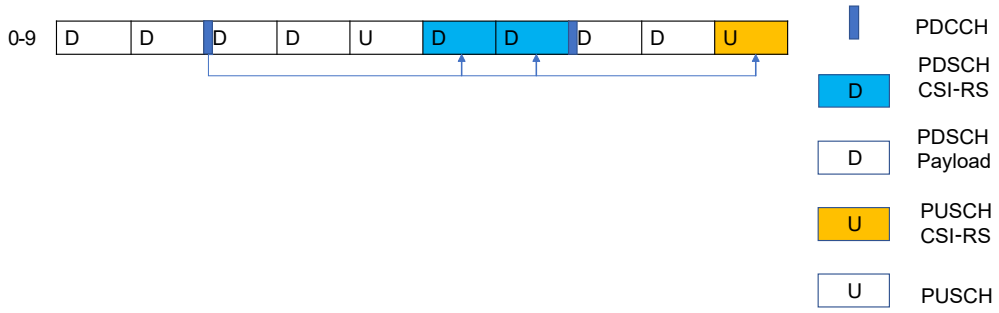

Figure 2.6: CSI-RS measurement sequence of 1 UE in 4-1 pattern

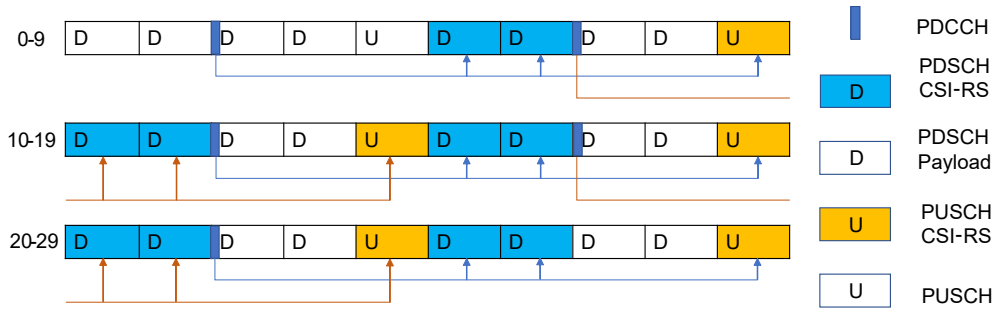

Figure 2.7: CSI-RS measurement sequence of 5 UEs in 4-1 pattern

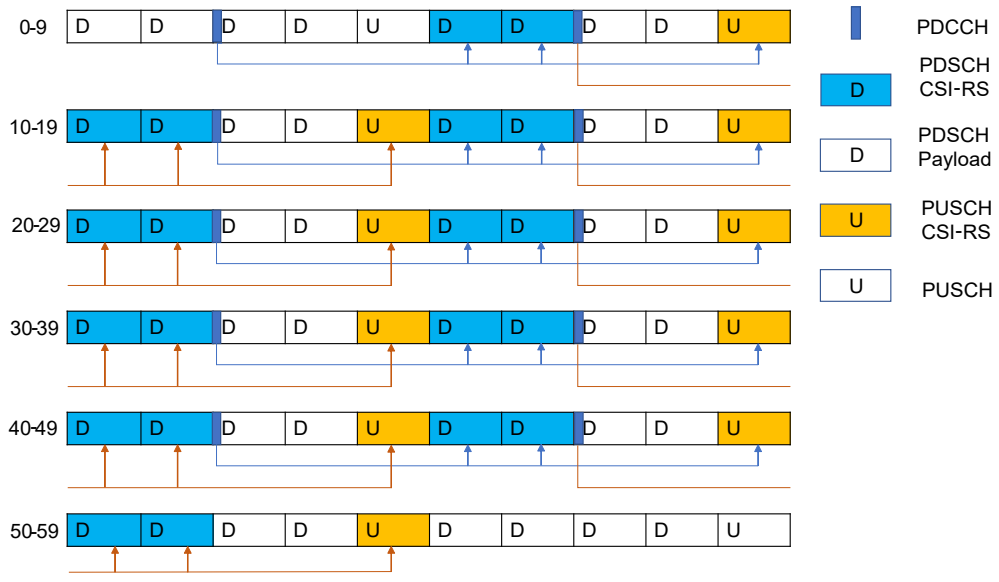

Figure 2.8: CSI-RS measurement sequence of 10 UEs in 4-1 pattern

For the 120khz OFDM subcarrier spacing system in Figure 2.9, the slot duration is 125μs. There are in total 320 slots. The SSB interval is by default 40ms. The theoretical maximum capacity are available for 64 UEs (128 CSI-RS PDSCH). However, not all the downlink (PDSCH) slots can be used for CSI-RS due to other physical channels like SSB and TRS (Tracking Reference Signal).

0-9 (160-169)	D	D	D	D	U	D	D	D	D	U
10-19 (170-179)	D	D	D	D	U	D	D	D	D	U
20-29 (180-189)	D	D	D	D	U	D	D	D	D	U
30-39 (190-199)	D	D	D	D	U	D	D	D	D	U
40-49 (200-209)	D	D	D	D	U	D	D	D	D	U
50-59 (210-219)	D	D	D	D	U	D	D	D	D	U
60-69 (220-229)	D	D	D	D	U	D	D	D	D	U
70-79 (230-239)	D	D	D	D	U	D	D	D	D	U
80-89 (240-249)	D	D	D	D	U	D	D	D	D	U
90-99 (250-259)	D	D	D	D	U	D	D	D	D	U
100-109 (260-269)	D	D	D	D	U	D	D	D	D	U
110-119 (270-279)	D	D	D	D	U	D	D	D	D	U
120-129 (280-289)	D	D	D	D	U	D	D	D	D	U
130-139 (290-299)	D	D	D	D	U	D	D	D	D	U
140-149 (300-309)	D	D	D	D	U	D	D	D	D	U
150-159 (310-319)	D	D	D	D	U	D	D	D	D	U

Figure 2.9: CSI-RS measurement sequence of 64 UEs in 120khz OFDM subcarrier spacing system (SSB interval 40ms)

For example, considering the above mentioned product configuration, only 50 UEs can be in connected mode. The Figure 2.10 and 2.11 shows that the total downlink capacity for payload is decreased due to the increased number of slots for CSI-RS with the increasing number of UEs.

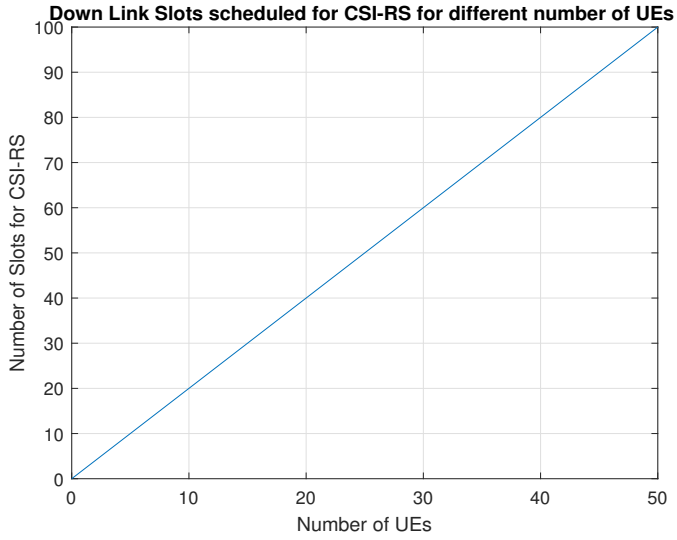

Figure 2.10: Down Link Slots scheduled for CSI-RS for different number of UEs

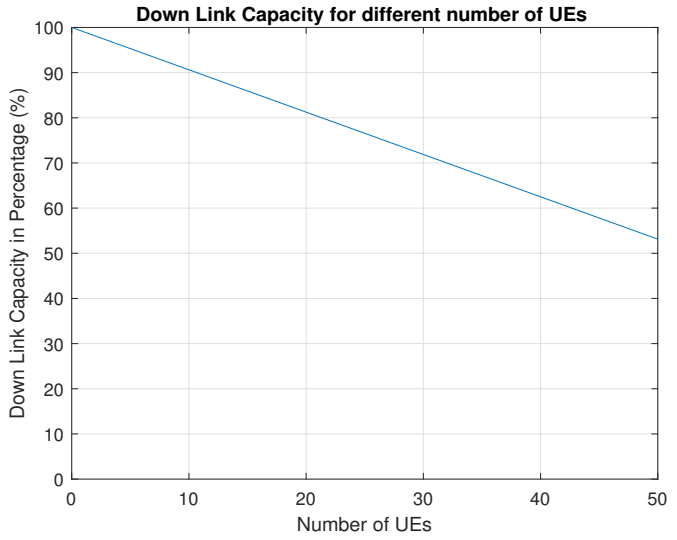

Figure 2.11: Down Link Capacity for different number of UEs

In Figure 2.11, the cell capacity with 50 connected UEs can be reduced almost by 50%.

Chapter 3

Machine Learning

3.1 Introduction

As a subsection of computer science, machine learning is originated from computational learning theory and pattern recognition in artificial intelligence. Machine learning focuses on the algorithms and construction which can make predictable function on data set. A model is created by making predictions from multiple inputs and output data sets [21].

3.1.1 Supervised Learning

In supervised learning, the learning process is performed by a function that can train a model from a big amount of input and output data (labeled data), then the model will be applied to new data to make prediction. The most known supervised learning methods are Neural network and decision tree.

3.1.2 Unsupervised Learning

In unsupervised learning, the model is not needed to be supervised by users. Unsupervised learning model can work itself to explore hidden structure that was undetected before. The dataset needed to be trained in unsupervised learning are unlabeled data. The most known unsupervised learning method is k-Means clustering.

3.1.3 Reinforcement Learning

In reinforcement learning, there is a cumulative reward or punishment for the input actions, so that the mapping of state is learnt. Compared to unsupervised learning which aims to get the similarity of dataset, the reinforcement learning finds out a good model that can maximize the whole cumulative reward of the agent. The most known reinforcement learning method is Q-learning.

3.2 Neural Network

Artificial neural networks (ANN) is inspired by the biological neural network from animal brains. A signal can be received by an artificial neuron and then be processed and transmitted to other neurons that connect to this neuron. There is a weight between neurons that adjusts as learning proceeds. The fluctuation of weight decides the connection strength of neurons. The neural network combines many different machine learning algorithms together rather than one independent algorithm.

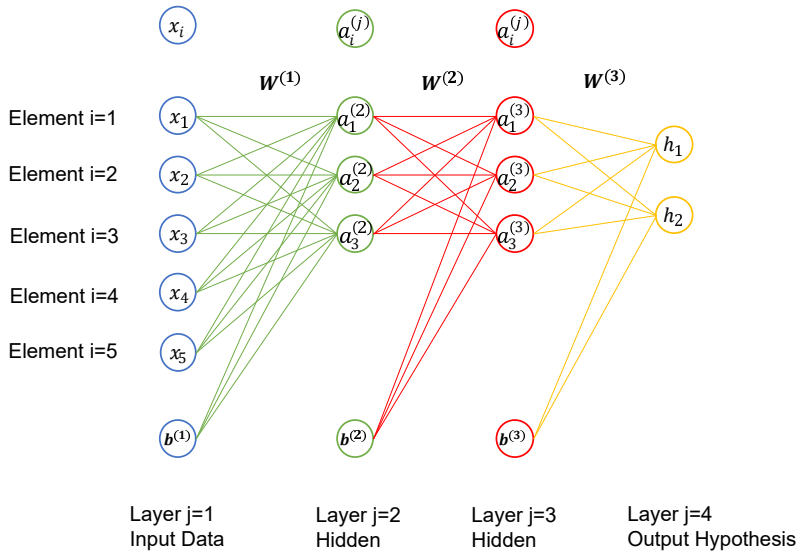

Figure 3.1: Neural Network Architecture

In Figure 3.1
i: the index of elements in each layer.

j: the index of layers.

x_i: input data.

$b^{(j)}$: bias unit in each layers.

$\Theta^{(j)}$ or $W^{(j)}$: matrix of weights controlling function mapping from layer j to layer j + 1.

$a_i^{(j)}$: "activation" of unit i in layer j.

h_i: the output hypothesis of the final output layer.

3.2.1 Forward Propagation

The input data follows the forward direction of the neural network. Neurons in hidden layers accept input data, then process it by the activation function and pass to the neurons in the next layer.

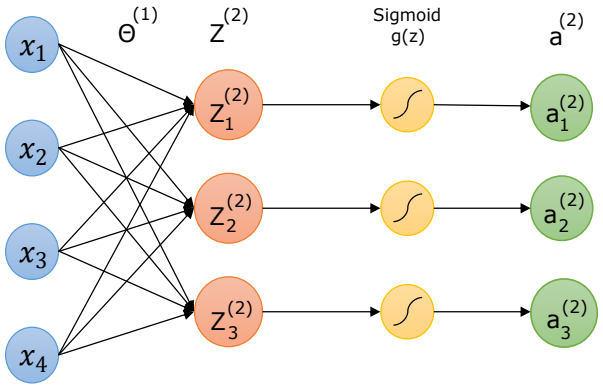

Figure 3.2: Neural Network Architecture

An example of one layer Vectorized Implementation of Forward Propagation in Figure 3.2:

$$x = \begin{bmatrix} x_1 \\ x_2 \\ x_3 \\ x_4 \end{bmatrix} \tag{3.1}$$

$$\Theta^{(1)} = \begin{bmatrix} \Theta_{10}^{(1)} & \Theta_{11}^{(1)} & \Theta_{12}^{(1)} & \Theta_{13}^{(1)} \\ \Theta_{20}^{(1)} & \Theta_{21}^{(1)} & \Theta_{22}^{(1)} & \Theta_{23}^{(1)} \\ \Theta_{30}^{(1)} & \Theta_{31}^{(1)} & \Theta_{32}^{(1)} & \Theta_{33}^{(1)} \end{bmatrix} \tag{3.2}$$

$$z_1^{(2)} = \Theta_{10}^{(1)} x_1 + \Theta_{11}^{(1)} x_2 + \Theta_{12}^{(2)} x_3 + \Theta_{13}^{(1)} x_4 \tag{3.3}$$

$$z_2^{(2)} = \Theta_{20}^{(1)} x_1 + \Theta_{21}^{(1)} x_2 + \Theta_{22}^{(2)} x_3 + \Theta_{23}^{(1)} x_4 \tag{3.4}$$

$$z_3^{(2)} = \Theta_{30}^{(1)} x_1 + \Theta_{31}^{(1)} x_2 + \Theta_{32}^{(2)} x_3 + \Theta_{33}^{(1)} x_4 \tag{3.5}$$

$$z^{(2)} = \begin{bmatrix} z_1^{(2)} \\ z_2^{(2)} \\ z_3^{(2)} \end{bmatrix} = \Theta^{(1)} x \tag{3.6}$$

$$g(z) = \frac{1}{1 + e^{-z}} \tag{3.7}$$

$$a^{(2)} = g(z^{(2)}) \tag{3.8}$$

For the Figure 3.2, this is a two hidden layers neural network. The forward propagation can be as followed calculation:

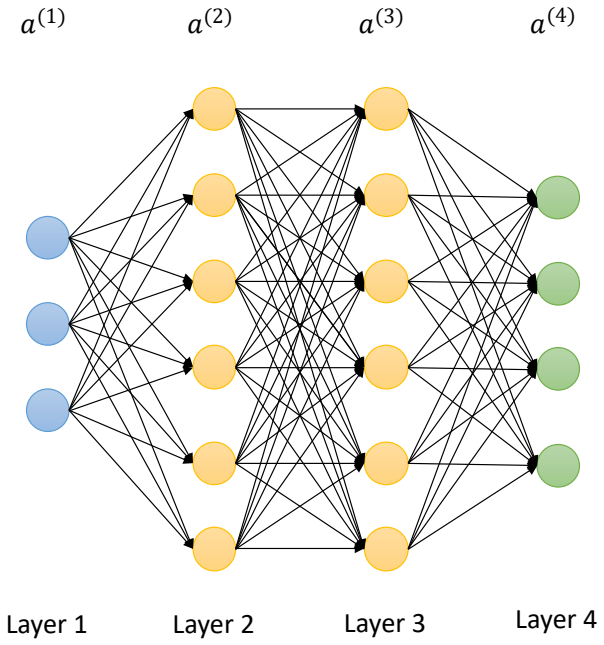

Figure 3.3: Two hidden layers Forward Propagation

$a^{(1)} = x$
$z^{(2)} = \Theta^{(1)} a^{(1)}$
$a^{(2)} = g(z^{(2)})$
$z^{(3)} = \Theta^{(2)} a^{(2)}$
$a^{(3)} = g(z^{(3)})$
$z^{(4)} = \Theta^{(3)} a^{(3)}$
$h_\Theta(x) = a^{(4)} = g(z^{(4)})$

3.2.2 Cost Function

The performance of machine learning can be shown by Cost Function. The difference (error) between expectation value and prediction value can be calculated by Cost Function in a form of single real number.

The regularized cost function for the neuron network is quite similar to the logistic regression cost function.

$$J(\Theta) = -\frac{1}{m}\left[\sum_{i=1}^{m}\sum_{k=1}^{K} y_k^{(i)} \log\left(h_\Theta(x^{(i)})_k\right) + (1 - y_k^{(i)} \log\left(1 - (h_\Theta(x^{(i)}))_k\right)\right] + \frac{\lambda}{2m}\sum_{l=1}^{L-1}\sum_{i=1}^{S_l}\sum_{j=1}^{S_{l+1}}(\Theta_{ji}^{(l))})^2 \tag{3.9}$$

m: number of samples
K: number of outputs
L: total number of layers
S_l: the number of units (not counting bias unit) in layer l.

3.2.3 Back Propagation

The back propagation follows the inverse direction of the whole neural network in order to calculate the gradient of cost function with respect to the weights of neural network. The value of weight is corrected every time in order to minimize the Cost Function value.

The Neural network in the Figure 3.3 can be used for the back propagation illustration.

$\delta_j^{(l)}$ denotes the "error" of node j in layer l.
For each output unit (layer L = 4) in Figure 3.3:

$$\delta_j^{(4)} = a_j^{(4)} - y_j \tag{3.10}$$

The vectorized form of equation 3.10 is:

$$\delta^{(4)} = a^{(4)} - y \tag{3.11}$$

$$\delta^{(3)} = (\Theta^{(3)})^T \delta^{(4)} .* g'(z^{(3)}) \tag{3.12}$$

$$\delta^{(2)} = (\Theta^{(2)})^T \delta^{(3)} .* g'(z^{(2)}) \tag{3.13}$$

In equation 3.12 and 3.13, $g^{'}$ denotes sigmoid gradient:

$$g^{'} = \frac{\partial}{\partial Z} g(Z) = g(Z)(1 - g(Z))) \tag{3.14}$$

and $g(Z)$ in equation 3.14 denotes $g(z) = \frac{1}{1+e^{-z}}$

From the equation 3.9, The partial derivative of cost function:

$$\frac{\partial}{\partial \Theta_{ij}^{(l)}} J(\Theta) = a_j^{(l)} \delta_i^{(l+1)} \tag{3.15}$$

3.2.4 Training

In order to have desired output, the weights and biased need to be optimized. This process is called training. In training, the Forward Propagation and Back Propagation are two main functions.

For training samples:

$$\left\{(x^{(1)}, y^{(1)}), (x^{(2)}, y^{(2)}), ..., (x^{(m)}, y^{(m)})\right\} \tag{3.16}$$

First Step: Set $k = 1 : m$, where m denotes the number of samples. Set $a^{(1)} = x^{(k)}$, The vectorized form is needed here. Perform Forward Propagation to compute $a^{(l)}$, where l denotes layers. $l = 2, 3, ..., L - 1$

Second Step:
Using $y^{(i)}$ to compute $\delta^{(L)} = a^{(L)} - y^{(i)}$. Then the $\delta^{(L-1)}$,$\delta^{(L-2)}$,...,$\delta^{(2)}$ can be computed by using formula 3.11-3.12.

Third Step:
Set $\Delta_{ij}^{(l)} = 0$, where Δ are the aggregated δ values for m training samples.

$$\Delta_{kj}^{(l)} = \Delta_{kj}^{(l)} + a_j^l \delta_k^{l+1} \tag{3.17}$$

or in vectorized form:

$$\Delta^{(l)} = \Delta^{(l)} + \delta^{l+1} (a^{(l)})^T \tag{3.18}$$

where T are matrix transpose.

$$D_{ij}^{(l)} = \frac{1}{m} \Delta_{ij}^{(l)} + \frac{\lambda}{m} \Theta_{ij}^{(l)} \tag{3.19}$$

$$\frac{\partial}{\partial \Theta_{ij}^{(l)}} J(\Theta) = D_{ij}^{(l)} \tag{3.20}$$

$$\Theta^{(l)} = \Theta^{(l)} - \alpha \frac{\partial}{\partial \Theta^{(l)}} J(\Theta) \tag{3.21}$$

$$b^{(l)} = b^{(l)} - \alpha \frac{\partial}{\partial b^{(l)}} J(\Theta) \tag{3.22}$$

3.2.5 Prediction

After multiple times training, The weights are computed to fit the samples. By doing forward propagation with trained weights, the output result is the desired one.

Chapter 4

Method

4.1 Simulator Data

The simulator is based on 3GPP baseline behaviour. It offers many important data which can be used to analyze the performance of algorithm. The available logs from simulator are listed:

- Coordination of UE
- Wide Beam Index
- Wide Beam RSRP Value
- Angle of Arrival value
- Timing Advance value (in the form of Distance)
- Narrow Beam Index
- Narrow Beam RSRP Value
- Throughput
- Block Error Rate

4.1.1 KPI Data

In order to compare the machine learning algorithm result with the simulator default 3GPP baseline algorithm, it is important to find the Key Performance Indicator as the comparison standard. The narrow beam RSRP value is the most vital KPI, which can shows how much the machine learning algorithm can fit to the Baseline. The throughput can be second crucial KPI, which demonstrates how much cell capacity gain can the machine learning algorithm bring.

4.1.2 Other Simulation Data

The other data are also important which can be used to analyze the behavior of baseline. For example, the UE coordinates and wide beam index can be used to find out the difference of wide beam radiation area size and the side lobe situation. In addition, the above data combination can also be used to check the moving pattern.

Some data like Block Error rate (BLER) can be another aspect to inspect the performance of machine learning algorithm, which is correlated to throughput. However, it will not be investigated in this thesis.

4.2 Method and Algorithm Overview

The goal of this thesis is to implement machine learning algorithm to the simulator in order to imitate the baseline behavior to predict narrow beam.

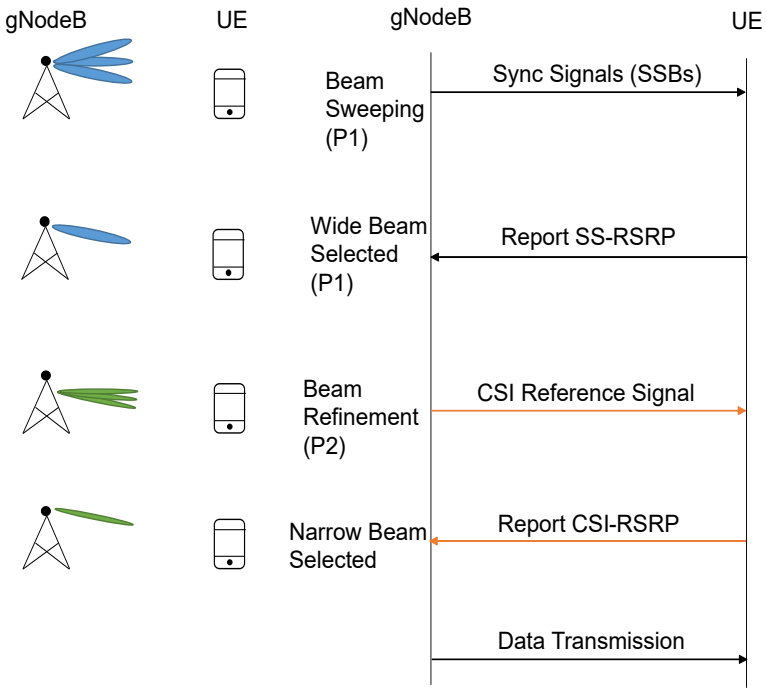

Figure 4.1: Baseline behavior

From the 3GPP, the beam management is performed in baseline as shown in the Figure 3.4. In P1, called beam sweeping, the SS blocks are broadcasted to UE in order to selected one wide beam with highest SS-RSRP value. Then for the decent data transmission, the narrow beam is needed in 5G NR. The P2 called beam refinement is proceed to select one narrow beam inside previous wide beam

by find out the highest CSI-RSRP value.
However, CSI-RS is scheduled for each UE and thus it consumes a lot of resource if many UE connected together.

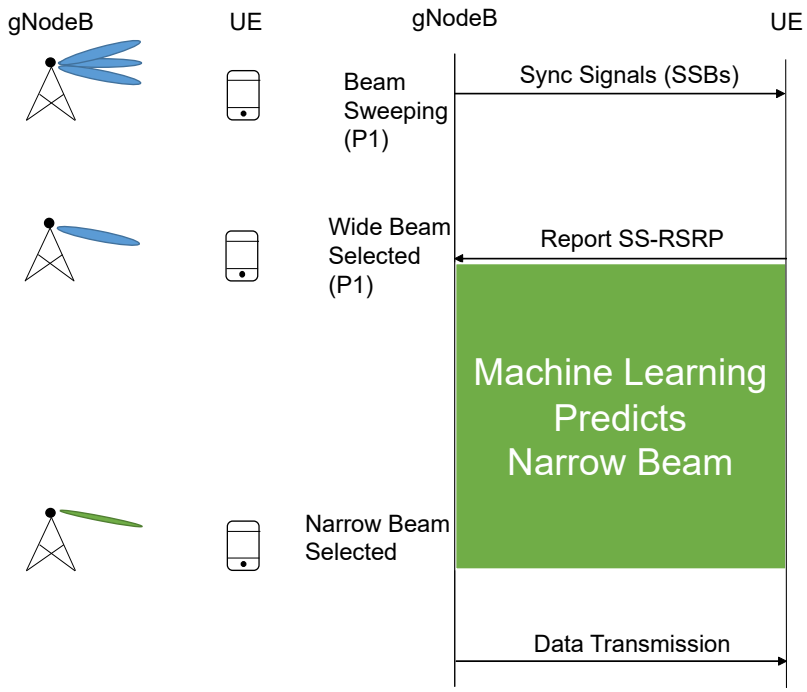

Figure 4.2: Machine Learning Method

The same as the baseline behavior, in P1 (beam sweeping), the SS blocks are broadcast to UE in order to selected one wide beam with highest SS-RSRP value. But then the machine learning takes over the beam refinement (P2 in baseline), and predict a narrow beam.

4.2.1 Training Data selection

The training data set is also very carefully selected, which can help machine learning to accurately predict the result and accelerate the training speed. In this thesis, the wide beam RSRP Values, angle of arrival value, timing advance value and narrow beam index are used to train the neural network.

After UE randomly moving in the hexagon cell area, UE coordinates, wide beam RSRP values, angle of arrival, timing advance data and narrow beam can be obtained from simulator logs data. Thus, the cell structure and wide beam radiation can be visualized in Figure 4.3.

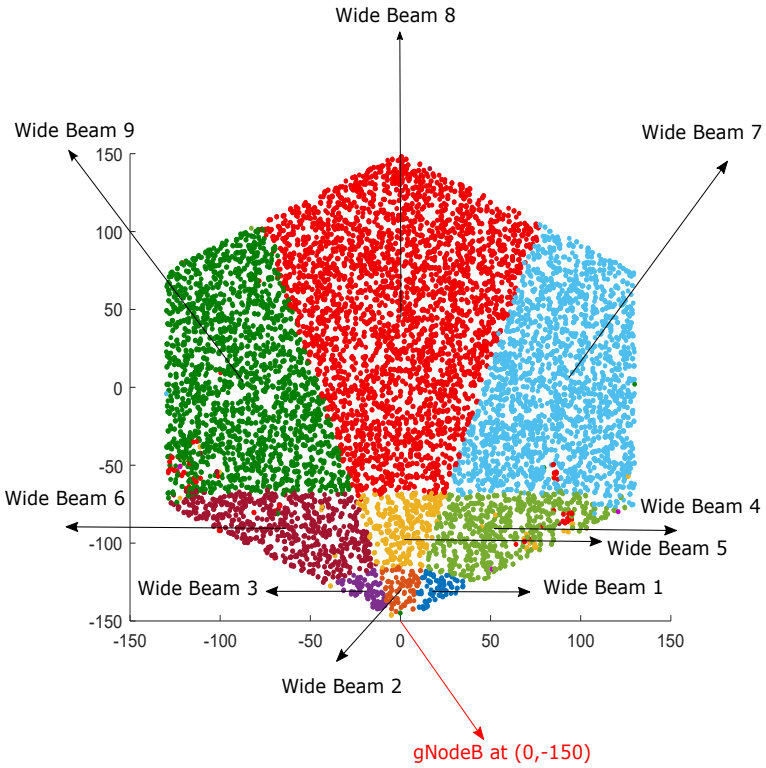

Figure 4.3: Wide beam distribution in the hexagon cell area

X	-1.505
Y	64.02
Time	34.02
RSRP1	-122.5
RSRP2	-103.4
RSRP3	-118.1
RSRP4	-113.5
RSRP5	-96.99
RSRP6	-112.1
RSRP7	-109
RSRP8	-90.47
RSRP9	-105.7
RSRP10	-114.9
RSRP11	-96.04
RSRP12	-110.3
BestWideBeam	8
BestNarrowBeam	8

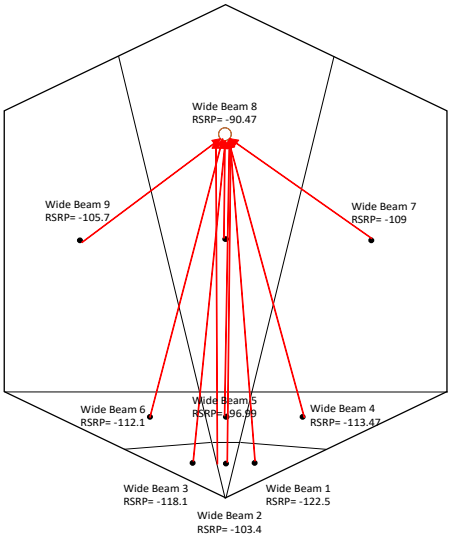

Figure 4.4: Co-Location by wide beam measurement

From Figure 4.3, The distribution of wide beams in a hexagon is not uniform. The hexagon in Figure 4.4 is a simplified version of the hexagon in Figure 4.3. In the wide beam 8, there is a UE at coordinate (-1.505,64.02), which has different wide beam RSRP values. Based on the path loss feature of wireless transmission, the further distance is the UE from the mainlobe wide beam radiation area(wide beam center), the less corresponding wide Beam RSRP value it has. Thus, the twelve wide beam RSRP values can be used to co-locate the relative "position" inside one wide beam coverage area. Then, the Narrow beam in a wide beam can be selected logically. In addition, the angle of arrival and timing advance value can be used for higher accuracy. In Figure 4.5, The narrow beam distribution is conceptually presented.

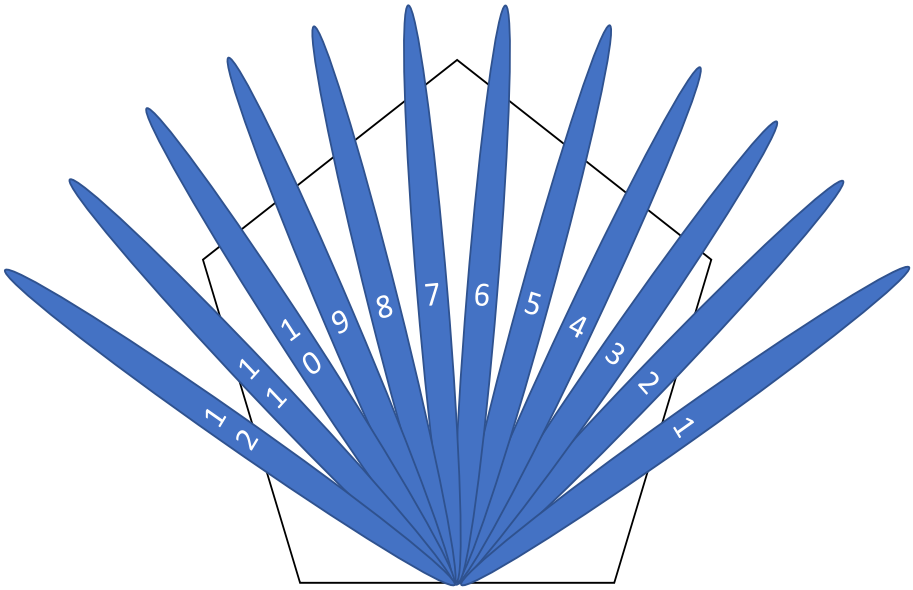

Figure 4.5: Conceptual Narrow beams drawn in Wide Beam 8 coverage area

4.3 Neural Network Training

the training data are selected in section 4.2. This section will introduce how the selected data are used for the Neural network training.

4.3.1 Input Layer

There are totally 15 row elements inside input matrix, which are 12 SSB rsrp values, AoA x-axis value, AoA y-axis value and timing advance value. The Equation 4.1 shows a m samples input matrix. For example, S1 denotes SSB RSRP value of wide beam 1. A_X and A_Y denote the azimuth value and elevation value of Angle of arrival. TA denotes the timing advance value.

$$\begin{bmatrix} S_1 & S_2 & S_3 & S_4 & S_5 & S_6 & S_7 & S_8 & S_9 & S_{10} & S_{11} & S_{12} & A_X & A_Y & T_A \\ \vdots & \cdots & \cdots & \cdots & \cdots & \cdots & \cdots & \cdots & \cdots & \cdots & \cdots & \cdots & \cdots & \cdots & \cdots \\ \vdots & \ddots & & & & & & & & & & & & & \\ \vdots & & \ddots & & & & & & & & & & & & \\ \vdots & & & \ddots & & & & & & & & & & & \\ \vdots & & & & \ddots & & & & & & & & & & \\ \vdots & & & & & \ddots & & & & & & & & & \\ \vdots & & & & & & \ddots & & & & & & & & \\ \vdots & & & & & & & \ddots & & & & & & & \\ \vdots & & & & & & & & \ddots & & & & & & \\ \vdots & & & & & & & & & \ddots & & & & & \\ \vdots & & & & & & & & & & \ddots & & & & \\ \vdots & & & & & & & & & & & \ddots & & & \\ \vdots & & & & & & & & & & & & \ddots & & \\ \vdots & & & & & & & & & & & & & \ddots & \\ \vdots & & & & & & & & & & & & & & \ddots \end{bmatrix} \tag{4.1}$$

4.3.2 Output layer

The row elements of output matrix are only narrow beam index. In this thesis we assume that there are totaly 12 narrow beams in one wide beam. The narrow beam index varies from 1 to 12. For the neural network training. the narrow beam index values are needed to be mapped to binary form. For example, narrow beam index "1" is mapped to [1 0 0 0 0 0 0 0 0 0 0 0], narrow beam index "12" is mapped to [0 0 0 0 0 0 0 0 0 0 0 1].

$$\begin{bmatrix} 1 & 0 & 0 & 0 & 0 & 0 & 0 & 0 & 0 & 0 & 0 & 0 \\ \vdots & \cdots & \cdots & \cdots & \cdots & \cdots & \cdots & \cdots & \cdots & \cdots & \cdots & \cdots \\ \vdots & \ddots & & & & & & & & & & \\ \vdots & & \ddots & & & & & & & & & \\ \vdots & & & \ddots & & & & & & & & \\ \vdots & & & & \ddots & & & & & & & \\ \vdots & & & & & \ddots & & & & & & \\ \vdots & & & & & & \ddots & & & & & \\ \vdots & & & & & & & \ddots & & & & \\ \vdots & & & & & & & & \ddots & & & \\ \vdots & & & & & & & & & \ddots & & \\ \vdots & & & & & & & & & & \ddots & \\ \vdots & & & & & & & & & & & \ddots \end{bmatrix}_{m \times 12} \tag{4.2}$$

4.3.3 Neural Network Training

Figure 4.6 shows the Training process of 4 layers Neural network, thus there are totally 3 weight matrix. After doing multiple times training (Combination of Forward Propagation and Back Propagation). The three desired weight matrix (W^1,W^2 and W^3) can be obtained.

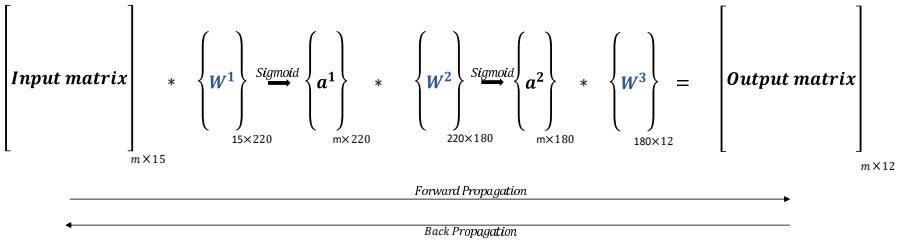

Figure 4.6: Neural Network Training Process

4.4 Simulation Flow

In this section, each step of simulation will be explained.

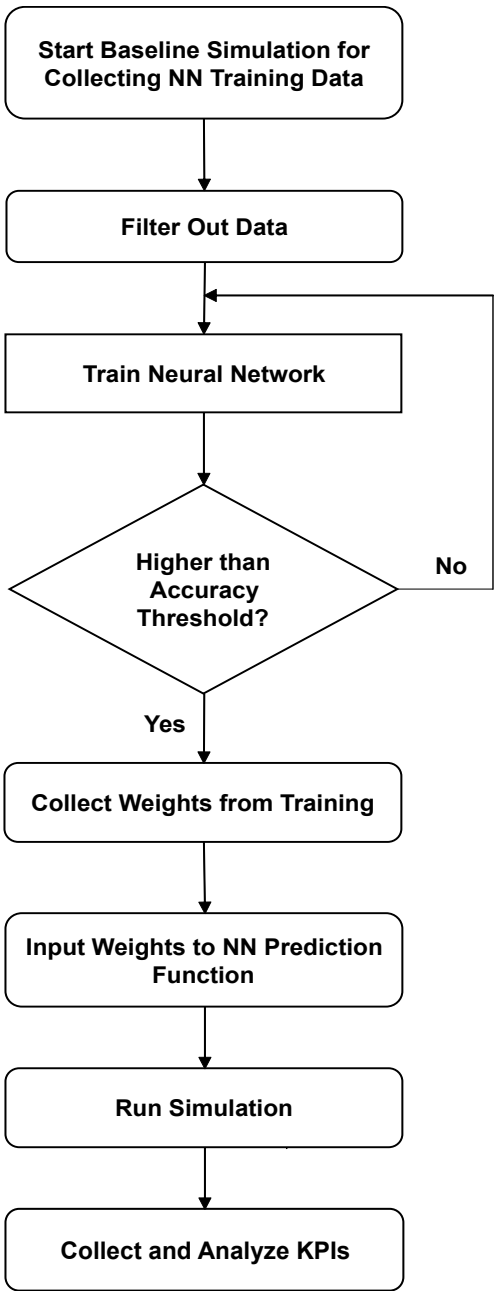

Figure 4.7: Simulation Flow Chart

- Step 1: Start baseline simulation for collecting neural network training data.

This step is done in the simulator in runtime. Modified configuration for the simulation is needed to get correct data. This configuration defines how the UE moves in the Cartesian plane, the UE speed etc.

- Step 2: Filter out data

The logging data is the mixture of letters and digital. It will be convenient to filter out the useful numbers (e.g. RSRP), which can be used for analyzing or training in Neural Network. This step is done in offline in MATLAB.

- Step 4: Train neural network

For increasing the algorithm's accuracy and the efficiency, the neural network has been trained in Matlab using a cloud server.

- Step 4: Collect weights from training.

After training, the weights of Neural network is collected in a CSV format matrix.

- Step 5: Input weights to neural network prediction function

The prediction function is implemented in JAVA and integrated in Simulator. The prediction function uses as core function the weights exported by the neural network training from step 3.

- Step 6: Run simulation

This step is done in the simulator in runtime, for different configurations, as at step 1. For comparison and evaluation, both baseline and neural network prediction function are needed to run in the simulator.

- Step 7: Collect and Analyze KPI

After having the data logs from both baseline and neural network prediction function, the data need to be filtered out (as at step 2) for the purpose of analysis. This step is done in offline in MATLAB.

Chapter 5

Simulation

5.1 Simulator environment

The Ericsson simulator is used in this thesis, which is a radio system models of radio network and users in terms of deployment, propagation, protocol and applications for different radio access technologies (RATs), including 5G NR, LTE, WIFI, WCDMA/HSPA. GSM/EDGE.
This simulator is written in Java, the core of simulator is a framework for any type of event-driven simulator with support for component hierarchies, parameter setting, logging etc, and developers can easily construct new types of simulators based on this core.

5.2 Basic Simulator Parameters

- **Carrier frequency:** 28 GHz
- **Bandwidth:** 100 MHz
- **Deployment scenario:** 1 cell with 1 base station
- **Cell shape:** Hexagon
- **Cell radius:** 150m
- **Number of cell sectors:** 3
- **Antenna height:** 25m
- **Number of antenna elements:** 128
- **Zenith angle:** 23°
- **Numerology:** 120KHz Sub-carrier Spacing
- **Number of widebeam:** 12
- **Number of narrowbeam:** 12 per widebeam

5.3 Specified Simulator Parameters

In this thesis, there are two scenarios were separately simulated, which are single UE scenario and Multiple UEs scenario. In this section, the specified parameters will be presented. The simulation was carried out for each wide beam, which means there are twelve training models for twelve wide beams inside one cell.

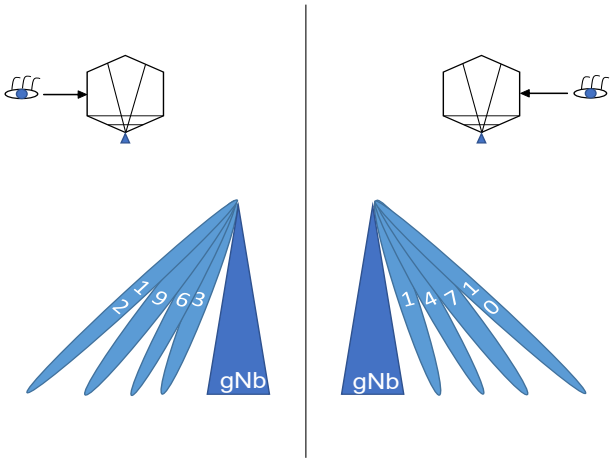

Figure 5.1: Wide beam 3D radiation

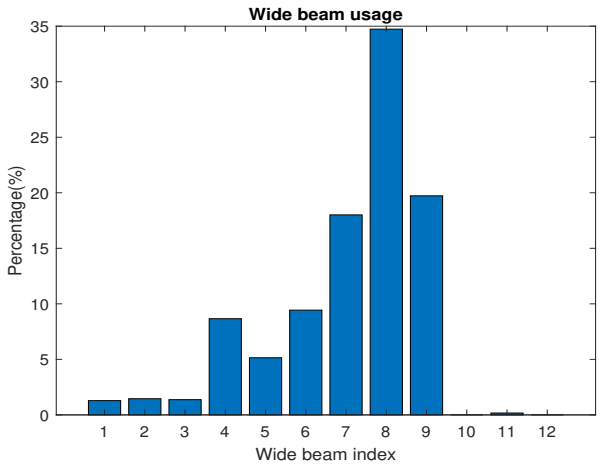

Figure 5.2: Wide beam distribution

The Figure 5.1 shows the 3D wide beam radiation of the simulator (the wide beam index 2, 5, 8, 11 were not plotted, please take Figure 4.3 as reference). The Figure 5.2 is the distribution plot of twelve wide beams inside a cell, this bar chart are plotted on the basis of the Figure 4.3 in Method chapter. The distribution of each

wide beam is not even from the setting of simulator, especially the wide beam index 10, 11 and 12 are very rare in the cell.

5.3.1 Simulator Seed

Seed is used to generate pseudo-random number. In simulator, the seed determines all the random parameter configurations. For example, the UE random movement pattern can be determined by the seed value. In addition, the seed is reproducible and can be hard coded manually. The seed must be hard coded to be same in simulation in order to make the comparison between machine learning algorithm and baseline.

5.3.2 Single UE scenario

For the single UE scenario, the accuracy is compared between machine learning algorithm and baseline. In order to collect as much as random positions inside one Hexagon, the random movement is the best choice for the UE moving pattern.

- **UE number:** 1
- **UE Height:** 1.5m
- **Movement:** Randomly moving in Hexagon cell.
- **Moving speed:** 1m/s
- **Number of seed for ML training:** 5
- **Number of seed for verification:** 1 (different from training seed)
- **Simulation duration:** 1000s

Random Mover

UE moves in a random direction with uniform distribution, and the pattern of random positions is determined by the seed. User locations will always be created inside the hexagon, movers will bounce back when hitting a circle that circumscribe the hexagon. The Figure 5.3 presents the random movement trajectory (5000 coordinates) of a single UE in a Cell.

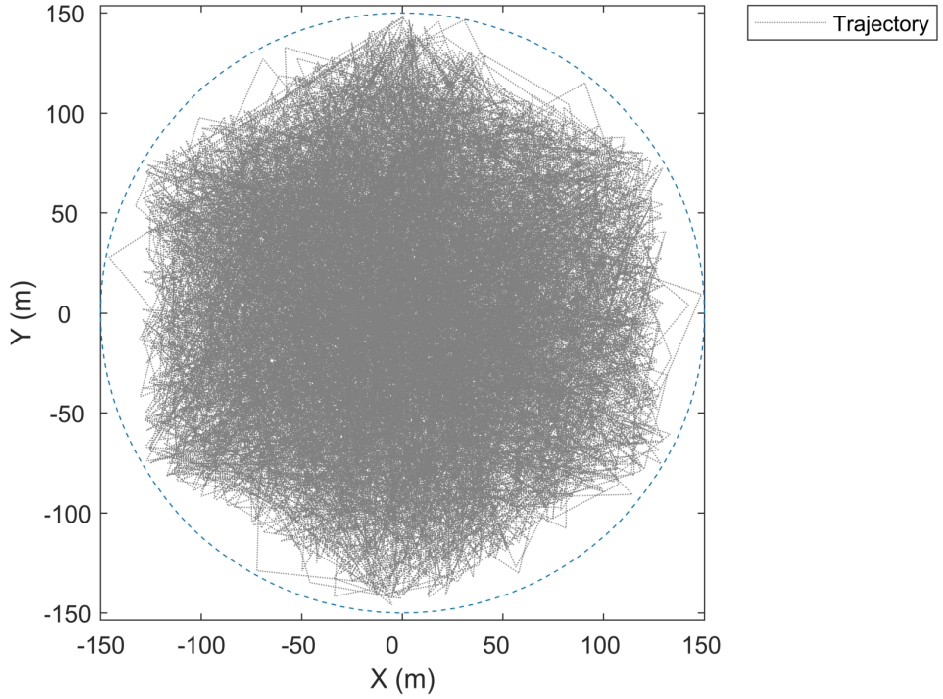

Figure 5.3: Random Mover Trajectory

5.3.3 Multiple UEs scenario

For the Multiple UEs scenario, the throughput is compared between machine learning algorithm and baseline. In order to force UE moving inside one wide beam, the circular UE movement were carried out in the simulation.

- **UE number:** [2,5,10,20,30,40]
- **UE height:** 1.5m
- **Movement:** Circular moving inside one wide beam.
- **Moving speed:** [1,5,10] m/s
- **Number of seed for ML training:** 5
- **Number of seed for verification:** 1 (different from training seed)
- **Simulation duration:** 50s

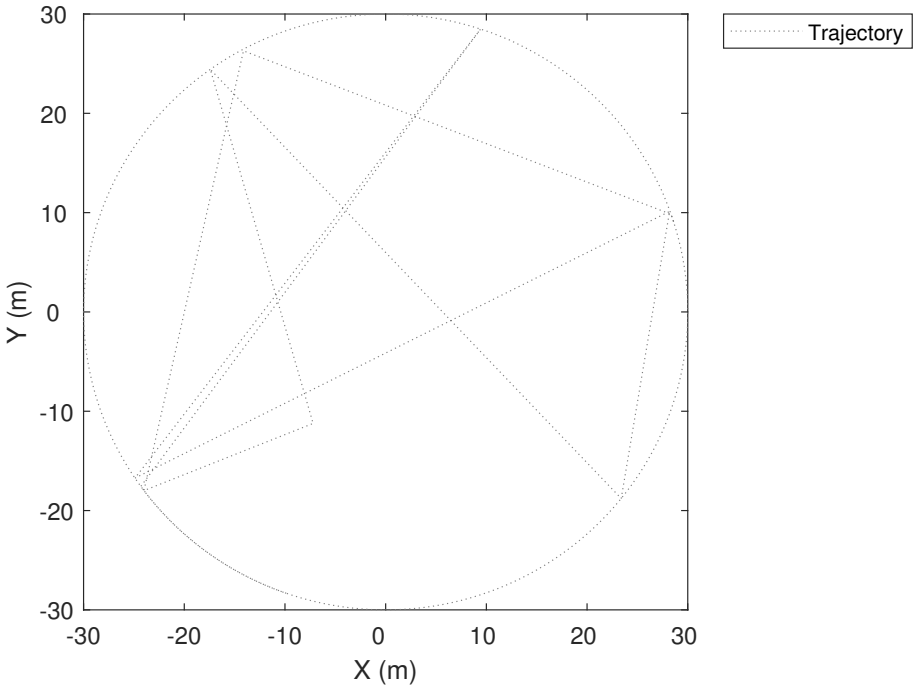

Figure 5.4: Circular Mover Trajectory

Circular Mover

UE moves randomly on the circle in the uniform distribution. The trajectory of UE movement are a circle with a preset coordinates as center point and a preset number as radius. In this simulation, the movement trajectory should always be inside one specific wide beam. For example, the Figure 5.4 presents the circular movement trajectory (at center point [0,0] with 30m radius) of 30 UEs inside wide beam 8.

5.4 Simulation KPIs

Simulation KPIs are used to compare the performance between machine learning algorithm and baseline. The KPIs consists of narrow beam index, narrow beam RSRP and throughput. In addition, some other logs from simulator are also important for the comparison in terms of visualization, such as UE moving coordinates.

5.4.1 Single UE scenario

For the single UE scenario, the performance comparison between algorithm and baseline are narrow beam index selection accuracy and narrow beam RSRP value gap.

Narrow beam index selection accuracy

The machine learning algorithm predicts a narrow beam index, meanwhile the baseline can also output a narrow beam index by having the CSI-RS enabled. These two narrow beam index selections are compared, so the accuracy of machine learning algorithm can be obtained.

$$\begin{cases} CorrectBeamPrediction, & \text{if } Difference = 0. \\ NeighborBeamPrediction, & \text{if } Difference = 1. \\ BadBeamPrediction, & \text{if } Difference > 1. \end{cases} \tag{5.1}$$

Narrow beam RSRP

The simulator can calculate a RSRP value on the basis of a narrow beam index. Thus, a RSRP value can be calculated by simulator after having a predicted narrow beam index by machine learning algorithm. By implementing probability density function, the RSRP value between algorithm and baseline can be compared.

5.4.2 Multiple UEs scenario

For the Multiple UEs scenario, the performance comparison between algorithm and baseline is done in terms of cell throughput. This throughput is relevant to the narrow beam RSRP value; the higher narrow beam RSRP value is, the higher throughput will be.

The average cell throughput is compared. But, there are three factors can influence the throughput value, which are number of UE, UE moving speed and SSB report interval. Thus, a different parameter combination is used for the simulator in order to obtain throughput.

- **UE numbers:** [2,5,10,20,30,40]
- **UE moving speed:** [1,5,10] m/s
- **SSB report interval:** [20,40] ms

For each second, each UE has a certain amount of throughput. Thus, the cell throughput is the sum of each individual UE throughput in this second. After several second simulation, the averaged cell throughput can be calculated. If the total number of UE is n, and the simulation duration is m sec.

$$AveragedCellThroughput = \frac{\sum_1^n \sum_1^m TP_n^m}{m} \tag{5.2}$$

For example, if the total number of UE is 2, and the running duration is 3 sec. Based on the Equation 5.2, the averaged throughput is: $\frac{TP_1^1+TP_2^1+TP_1^2+TP_2^2+TP_1^3+TP_2^3}{3}$.

Chapter 6

Result

In this chapter, the result from simulator and the performance between machine learning algorithm and baseline will be compared. Note: The result is mainly focused on wide beam eight, the same can be done for other wide beams.

6.1 Single UE scenario

For the single UE scenario, three KPIs were evaluated in the simulation, which are narrow beam index and RSRP value. There are two way to demonstrate the accuracy of machine learning algorithm. The first one is to compare the narrow beam index at a certain coordinates. The second one is to compare the fitting curve of Probability density function (PDF) of RSRP value.

For the validation of machine learning algorithm, unique seed was used for the simulation of machine learning algorithm and baseline, which can guarantee the UE moving pattern of machine learning algorithm are the same as baseline.

In Figure 6.1, the prediction result of neural network are compared with baseline inside wide beam eight. A number of 9126 simulation samples inside the wide beam eight are examined. The blue dots represent the correct predictions of narrow beam index, the green dots represent the neighbour narrow beam predictions, and the red dots represent the bad narrow beam predictions. The percentage of correct prediction is 79.4324% (7249 samples), The percentage of neighbouring prediction is 18.6610% (1703 samples), and the percentage of bad narrow beam prediction is 1.9066% (174 samples). The selection of narrow beams on side lobes are mostly "wrong" predictions.

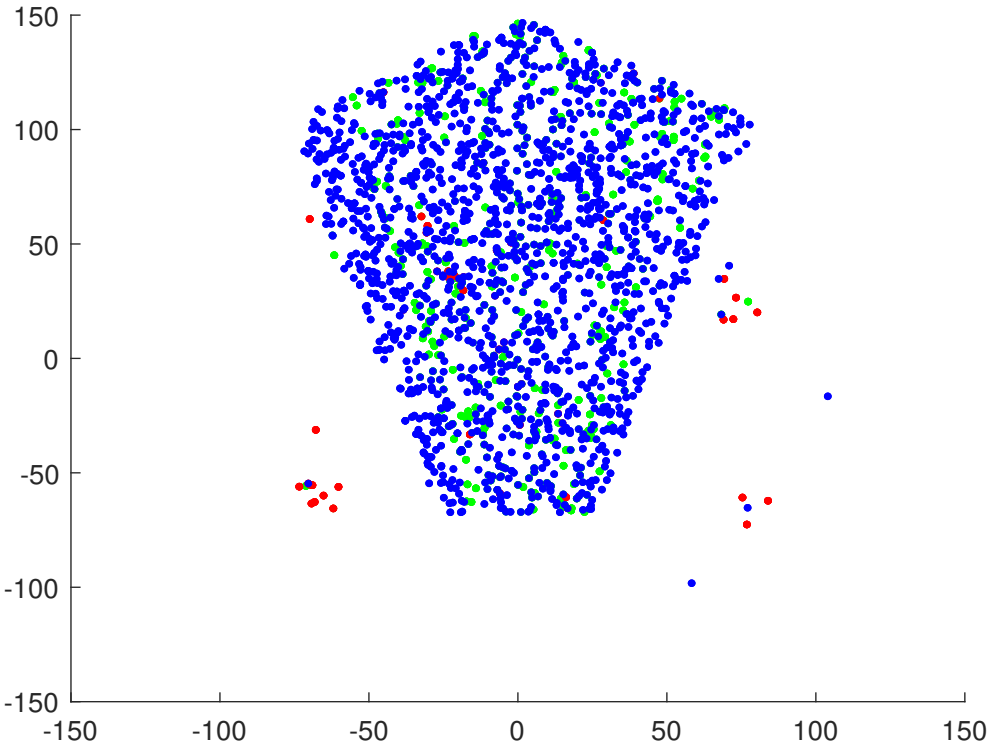

Figure 6.1: Accuracy of Neural network for UE at random positions

The Figure 6.2 and Figure 6.3 presents each narrow beam inside wide beam eight. There are twelve colors, which correspond to twelve narrow beams.

The Figure 6.2 shows the baseline narrow beam distribution inside wide beam eight. The picture aims to presents the boundary between different narrow beam areas, which is used to compare with the result of machine learning algorithm. In this picture, there are clear boundaries between narrow beam clusters.

The Figure 6.3 shows the narrow beam distribution from neural network simulation. Comparing with baseline, the narrow beam clusters in Figure 6.3 may not be clearly divided like baseline in Figure 6.2. Overall, the narrow beam distribution are quite similar between neural network and baseline, although there are some unclear boundaries due to the relative high percentage of neighbouring narrow beam prediction (18.6610%).

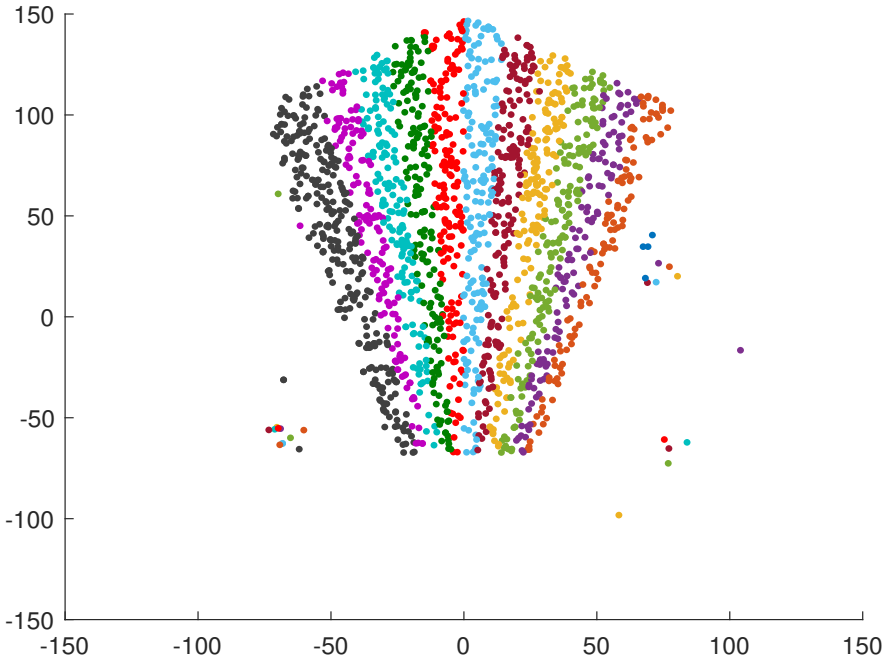

Figure 6.2: Baseline narrow beam distribution

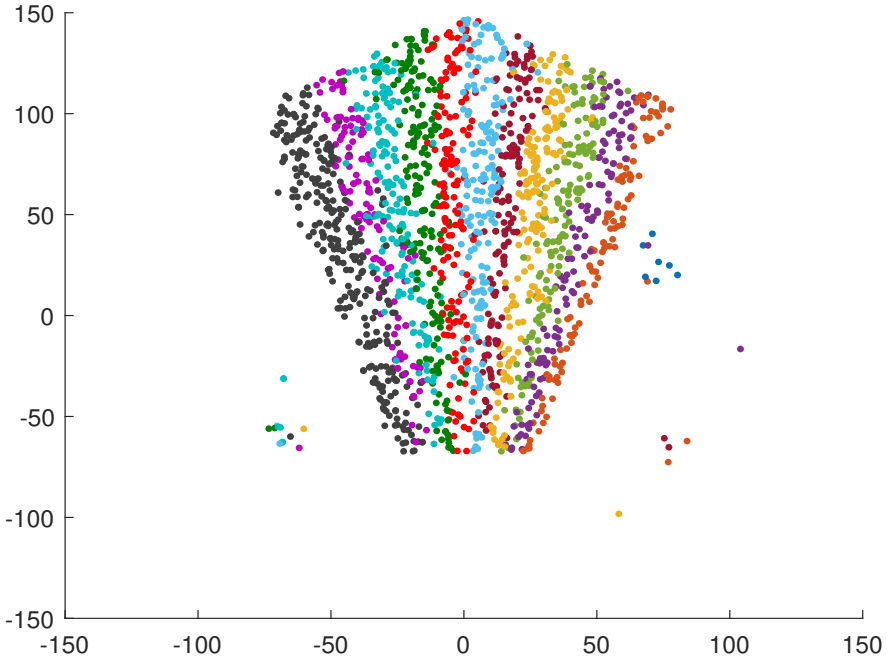

Figure 6.3: The distribution of narrow beam predicted by Neural network

The Figure 6.4 demonstrates the Probability density function (PDF) of RSRP values for Neural network and baseline. There are some low RSRP value(green bar chart) distributed on the left side of the plot due to some bad narrow beam predictions by neural network. Consequently, the fitting curve of neural network data slightly shifts to the left compared with fitting curve of base line. However, the gap of average RSRP values between neural network data set and baseline data set is only 0.8dB. This RSRP drop could impact the throughput but it could be leveraged by the gain in slots, which the neural network releases.

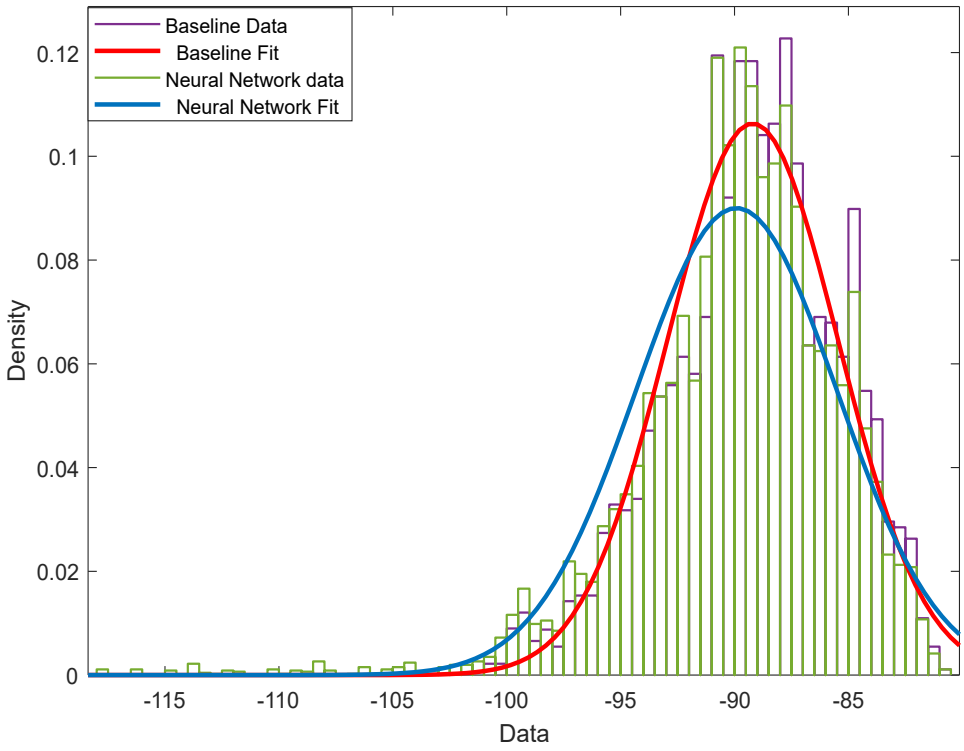

Figure 6.4: PDF of RSRP values of Neural network and Baseline

6.2 Multiple UEs scenario

For the Multiple UEs scenario, only one KPI was extracted in the simulation, which is throughput. The throughput is determined by three factors, which are number of UEs, UE moving speed and SSB report interval. The average throughput of the different setting combinations will be compared.

The Figure 6.5 shows the throughput comparison between neural network algorithmand baseline on condition of UE speed 1m/s and 40ms SSB report interval. As can be seen in this figure, the averaged throughput of neural network has the same trend as the baseline. And there is a noticeable throughput increase when the number of UEs is 2, 5 and 10. Then there is a huge throughput gain when the number of UEs is 20, 30 and 40. The reason behind the high throughput gain is: for the baseline, with the increasing number of UEs connected to the cell, there are more DL time slots allocated for the CSI-RS. In comparison, the neural network can predict narrow beam without using any mentioned time slots. Consequently, more DL time slots can be used for the payload.

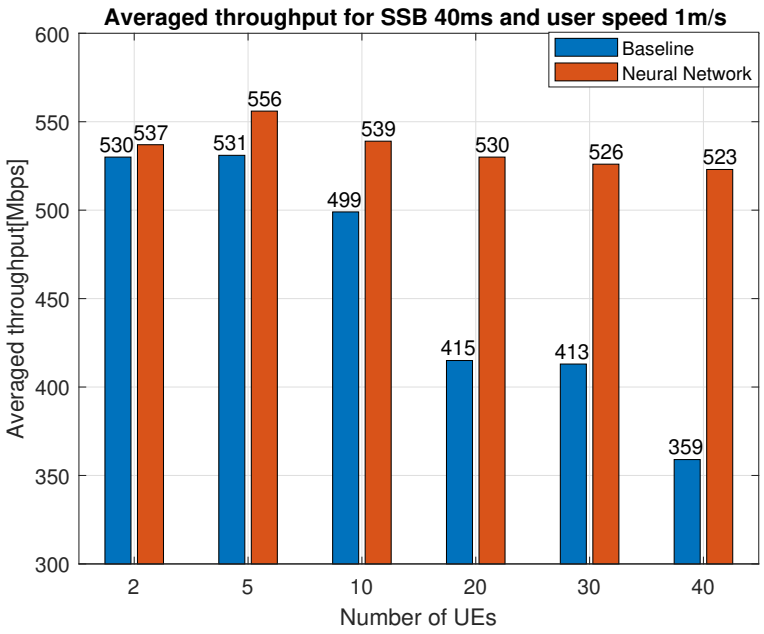

Figure 6.5: Averaged cell throughput for UE speed 1m/s

The Figure 6.5 shows the throughput comparison between neural network algorithm and baseline on condition of UE speed 5 m/s and 40ms SSB report interval. In comparison with the Figure 6.5, the Figure 6.6 has the similar result and trend, but the averaged throughput is relatively lower due to the higher UE moving speed.

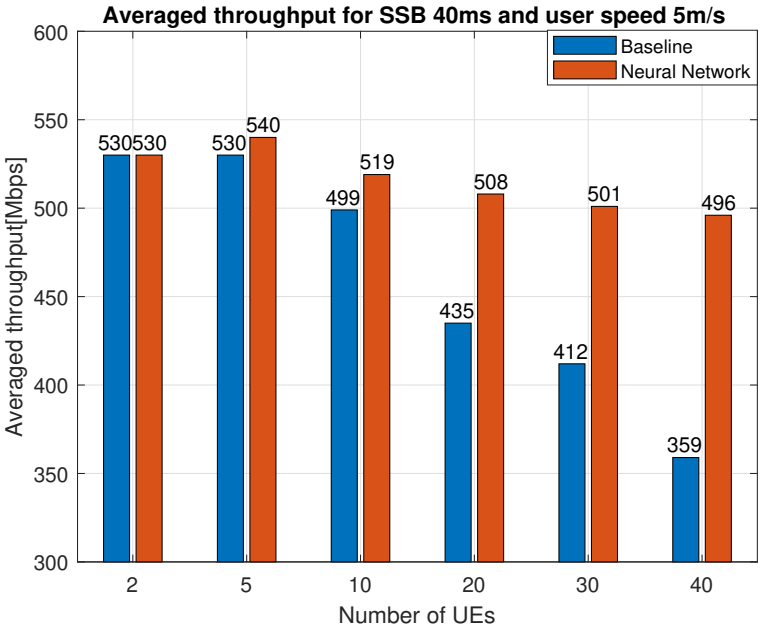

Figure 6.6: Averaged cell throughput for UE speed 5m/s

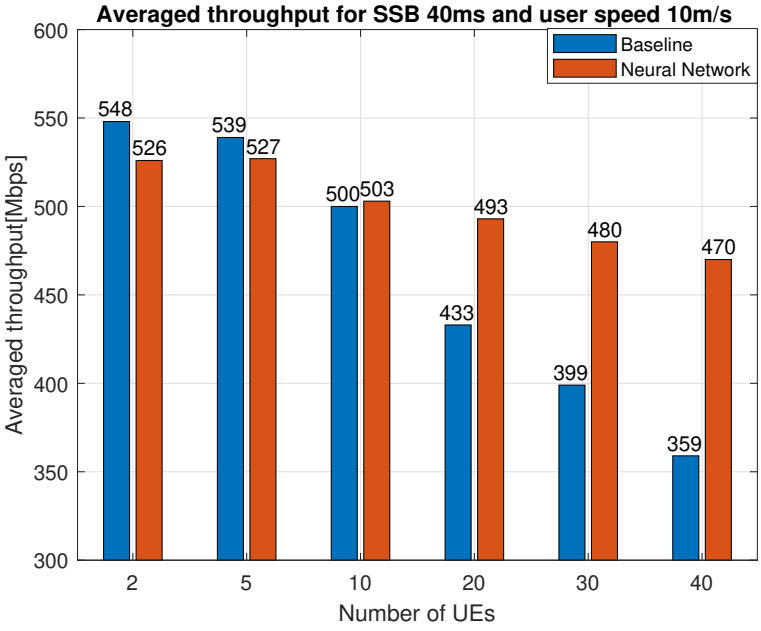

Figure 6.7: Averaged cell throughput for UE speed 10m/s

In Figure 6.7, there is a noticeable throughput performance drop compared to Figure 6.5 and Figure 6.6. The neural network has a worse result compared to baseline when there are 2 or 5 UEs connected to the cell. The reason for the performance drop is: for the 40ms SSB report interval, the gNb can not accurately report the on time RSRP value to the neural network prediction function when the UE speed is high. Thus the prediction will sometimes select a non-optimal narrow beam, which lower the narrow beam RSRP value. Consequently, the cell throughput is lower.

In order to solve the problem in Figure 6.7. The shorter SSB report interval is adapted. The Figure 6.8 shows the throughput comparison between neural network algorithm and baseline on condition of UE speed 10m/s. For the 20ms SSB interval, the neural network has a considerable throughput gain compare to the result of 40ms SSB interval. However, for the baseline, the shorter SSB report interval can reduce the supportive UE number in a cell. The 20ms SSB interval can only support half amount of UE number in a cell compared with the 40ms SSB report interval.

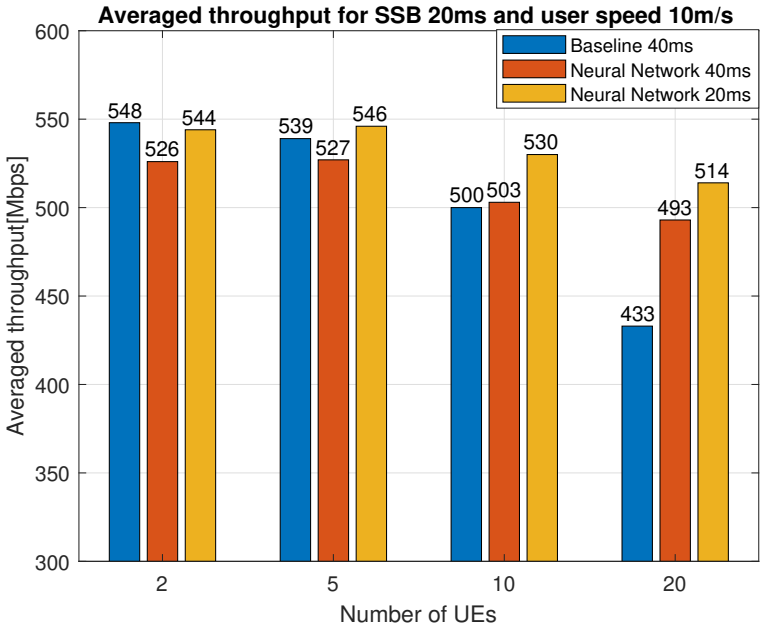

Figure 6.8: Averaged cell throughput for 20ms SSB report interval and UE speed 10m/s

Chapter 7

Conclusion

7.1 Overall results

The overall result of thesis shows that the machine learning algorithm can imitate the baseline behaviour. For static environment, the machine learning has very high accuracy in terms of narrow beam prediction with a extremely low average RSRP drop in comparison with baseline. For the moving environment, the machine learning has a surprisingly high cell throughput growth for more connected UEs. In the high speed environment, the machine learning has a acceptable throughput performance.

7.2 Future work

Due to the limitation of the time, some aspects are not covered in this thesis. Firstly, this thesis in mainly focus on line-of-sight transmission. It would be good that the models and methods can be modified for the NLOS scenario in the future. Secondly, the machine learning algorithm may not perform good for all of the seeds due to the calculation complexity. It can be a good choice that more data sets from more seeds can be used for machine learning training, which should have a better result when moving environment changes.

References

[1] X. Zhou, V. FAKHOURY, "User Equipment Characterization using Machine Learning", M.S. thesis, Dept. Elect. Eng., Lund Univ., Lund, Sweden, 2019.

[2] B. Joel, F. Gustav, "Machine Learning Technique for Beam Management in 5G NR RAN at mmWave Frequencies", M.S. thesis, Dept. Elect. Eng., Lund Univ., Lund, Sweden, 2019.

[3] W. Na, B. Bae, S. Cho and N. Kim, "Deep-learning Based Adaptive Beam Management Technique for Mobile High-speed 5G mmWave Networks", 2019 IEEE 9th International Conference on Consumer Electronics (ICCE-Berlin), Berlin, Germany, 2019, pp. 149-151, doi: 10.1109/ICCE-Berlin47944.2019.8966183.

[4] F. Boccardi, R. W. Heath, A. Lozano, T. L. Marzetta and P. Popovski, "Five disruptive technology directions for 5G", in IEEE Communications Magazine, vol. 52, no. 2, pp. 74-80, February 2014, doi: 10.1109/MCOM.2014.6736746.

[5] M. Giordani, M. Polese, A. Roy, D. Castor and M. Zorzi, "A Tutorial on Beam Management for 3GPP NR at mmWave Frequencies", in IEEE Communications Surveys Tutorials, vol. 21, no. 1, pp. 173-196, Firstquarter 2019, doi: 10.1109/COMST.2018.2869411.

[6] E. Ove, S. Magnus, van de Beek, J-J., L. Daniel and S. Frank, "An introduction to orthogonal frequency-division multiplexing", (Div. of Signal Processing, Research Report; Vol. TULEA 1996:16). Luleå University of Technology.

[7] A. A. Zaidi et al., "Waveform and Numerology to Support 5G Services and Requirements", in IEEE Communications Magazine, vol. 54, no. 11, pp. 90-98, November 2016, doi: 10.1109/MCOM.2016.1600336CM.

[8] G. Sanfilippo, O. Galinina, S. Andreev, S. Pizzi, G. Araniti, "A Concise Review of 5G New Radio Capabilities for Directional Access at mmWave Frequencies", In: Galinina O., Andreev S., Balandin S., Koucheryavy Y. (eds)

Internet of Things, Smart Spaces, and Next Generation Networks and Systems. NEW2AN 2018, ruSMART 2018. Lecture Notes in Computer Science, vol 11118. Springer, Cham.

[9] J. Lee, J.K. Han and J. Zhang, "MIMO Technologies in 3GPP LTE and LTE-Advanced", J Wireless Com Network 2009, 302092 (2009).

[10] Ericsson, "Advanced antenna systems for 5G networks", White paper

[11] J. Cavazos, D.McGrath and N. Faubert, "Engineering the 5G World: Design and Test Insights", Keysight Technologies 2020.

[12] 5G Americas, "5G Americas White Paper: Advanced Antenna Systems for 5G", white paper

[13] V. Va, H. Vikalo and R. W. Heath, "Beam tracking for mobile millimeter wave communication systems", 2016 IEEE Global Conference on Signal and Information Processing (GlobalSIP), Washington, DC, 2016, pp. 743-747, doi: 10.1109/GlobalSIP.2016.7905941.

[14] F.Afroz, R. Subramanian, R. Heidary, K. Sandrasegaran and S. Ahmed, "SINR, RSRP, RSSI and RSRQ Measurements in Long Term Evolution Networks" (2015)

[15] S. Ahmadi, "5G NR: Architecture, Technology, Implementation, and Operation of 3GPP New Radio Standards", 2019, pp. 506-512

[16] A. Omri, M. Shaqfeh, A. Ali and H. Alnuweiri, "Synchronization Procedure in 5G NR Systems", in IEEE Access, vol. 7, pp. 41286-41295, 2019, doi: 10.1109/ACCESS.2019.2907970.

[17] E. Dahlman, S. Parkvall and J. Sköld, "4G LTE-Advanced Pro and The Road to 5G (Third Edition)", 2016, pp. 269-283

[18] A. Badawy, T. Khattab, D. Trinchero, T. ElFouly and A. Mohamed, "A Simple Angle of Arrival Estimation System", 2017 IEEE Wireless Communications and Networking Conference (WCNC), San Francisco, CA, 2017, pp. 1-6, doi: 10.1109/WCNC.2017.7925867.

[19] S. Mukherjee, A. K. Sinha and S. K. Mohammed, "Timing Advance Estimation and Beamforming of Random Access Response in Crowded TDD Massive MIMO Systems", in IEEE Transactions on Communications, vol. 67, no. 6, pp. 4004-4019, June 2019, doi: 10.1109/TCOMM.2019.2900242.

[20] J. Acharya, L. Gao and S. Gaur, "LTE Signal Structure and Physical Channels", in Heterogeneous Networks in LTE-Advanced , Wiley, 2014, pp.45-71, doi: 10.1002/9781118693964.ch3.

[21] KNOX, S. W. (2018). Machine learning: a concise introduction.